INTERNATIONAL JOURNAL FOR NUMERICAL METHODS IN FLUIDS
Int. J. Numer. Meth. Fluids 2002; **38**:769–788 (DOI: 10.1002/fld.243)

Numerical solutions of the shallow water equations with discontinuous bed topography

J. G. Zhou*,†, D. M. Causon, D. M. Ingram and C. G. Mingham

Centre for Mathematical Modelling and Flow Analysis, The Manchester Metropolitan University, Manchester M1 5GD, U.K.

SUMMARY

A simple scheme is developed for treatment of vertical bed topography in shallow water flows. The effect of the vertical step on flows is modelled with the shallow water equations including local energy loss terms. The bed elevation is denoted with z_b^- for the left and z_b^+ for the right values at each grid point, hence exactly representing a discontinuity in the bed topography. The surface gradient method (SGM) is generalized to reconstruct water depths at cell interfaces involving a vertical step so that the fluxes at the cell interfaces can accurately be calculated with a Riemann solver. The scheme is verified by predicting a surge crossing a step, a tidal flow over a step and dam-break flows on wet/dry beds. The results have shown good agreements compared with analytical solutions and available experimental data. The scheme is efficient, robust, and may be used for practical flow calculations. Copyright © 2002 John Wiley & Sons, Ltd.

KEY WORDS: bed discontinuity; surface gradient method; shallow water equations; data reconstruction; high resolution method; Godunov method

1. INTRODUCTION

Several high-resolution Godunov-type methods have been developed to solve the shallow water equations with source terms such as bed slope and bed shear stress, demonstrating the accuracy, effectiveness and robustness of such methods. Bermudez and Vázquez [1] proposed an upwind method for shallow water equations with bed slope source term and Vázquez-Cendón [2] applied the same idea to solve more shallow water flow problems. However, their scheme is complex. LeVeque [3] developed a treatment for the bed slope source term which balanced source terms and flux gradients. The method can provide an accurate solution for a quasi-steady problem, but it is difficult to apply to steady transcritical flow with shock waves. Recently, Hubbard and Garcia-Navarro [4] proposed a scheme balancing source terms and flux gradients, in which the upwind method of Bermudez and Vázquez is used for source terms.

*Correspondence to: J. G. Zhou, Department of Computing and Maths, The Manchester Metropolitan University, Manchester M1 5GD, U.K.
†E-mail: J.G.Zhou@mmu.ac.uk

Received 28 February 2001
Revised 11 July 2001

In the literature, research on Godunov-type methods for shallow water flows involving a vertical step is very limited. This may be because (i) the shallow water equations are not valid in the region of vertical step where the effect of local non-hydrostatic pressure is significant, and (ii) it is difficult to represent a vertical step in a numerical algorithm. Hu *et al.* [5] used a very steep slope to replace a vertical step; hence a fine mesh must be used locally to resolve the steep slope. However, this is not a true representation of a vertical step although the solution is acceptable.

More recently, the authors have developed a surface gradient method (SGM) [6] for the shallow water equations with source terms such as bed slope. The scheme is simple, efficient and accurate. All source terms can be naturally and simply discretized with a centred scheme. This greatly simplifies programming and saves computer effort. However, the SGM cannot be applied directly to shallow water flows over a vertical step. In this paper, we describe a general scheme for shallow water flows over a vertical step, by extending the SGM. The scheme is used to simulate several test problems. The numerical results are compared with analytical solution and experimental data.

2. 2D SHALLOW WATER EQUATIONS

The 2D shallow water equations with source terms may be written in vector form as,

$$\frac{\partial \mathbf{U}}{\partial t} + \nabla \cdot \mathbf{F} = \mathbf{S} \tag{1}$$

where $\mathbf{U}$ is the vector of conserved variables, $\mathbf{F}$ is the flux vector function and $\mathbf{S}$ is the vector of source terms, and $\nabla = \vec{i}(\partial/\partial x) + \vec{j}(\partial/\partial y)$ is the gradient operator. $\mathbf{U}$, $\mathbf{F}$ are

$$\mathbf{U} = \begin{pmatrix} \phi \\ \phi u \\ \phi v \end{pmatrix}, \qquad \mathbf{F} = \begin{pmatrix} \phi \mathbf{V} \\ \phi u \mathbf{V} + \frac{1}{2}\phi^2 \vec{i} \\ \phi v \mathbf{V} + \frac{1}{2}\phi^2 \vec{j} \end{pmatrix} \tag{2}$$

and $\mathbf{S} = \mathbf{S}_b + \mathbf{S}_f$ with

$$\mathbf{S}_b = \begin{pmatrix} 0 \\ g\phi \dfrac{\partial H}{\partial x} \\ g\phi \dfrac{\partial H}{\partial y} \end{pmatrix}, \qquad \mathbf{S}_f = \begin{pmatrix} 0 \\ -\dfrac{g}{\rho}\tau_{fx} \\ -\dfrac{g}{\rho}\tau_{fy} \end{pmatrix} \tag{3}$$

where $\phi = gh$ is the geopotential, $g = 9.81\ \mathrm{m\ s^{-2}}$ is the acceleration due to gravity, ρ is the water density, h is the water depth, H is the partial depth between a fixed reference level and the bed surface (see definition sketch in Figure 1 for the 1D case), u and v are the x and y components of flow velocity, respectively, $\mathbf{V}$ is the velocity vector defined by $\mathbf{V} = u\vec{i} + v\vec{j}$, $\mathbf{S}_b$ is the bed slope term and $\mathbf{S}_f$ is the bed shear stress term with x and y components defined by depth-averaged velocities,

$$\tau_{fx} = \rho C_f u\sqrt{u^2 + v^2}, \qquad \tau_{fy} = \rho C_f v\sqrt{u^2 + v^2} \tag{4}$$

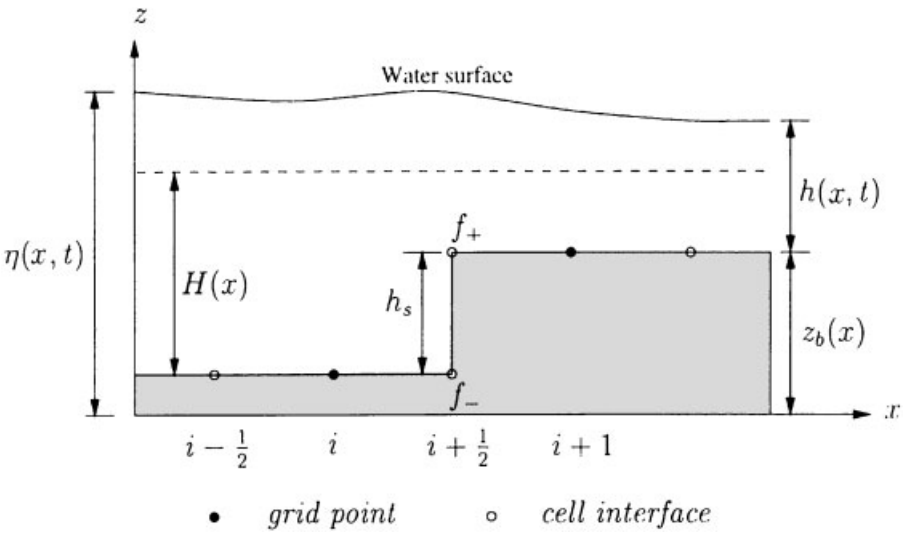

Figure 1. Definition sketch for vertical step.

where C_f is the bed friction coefficient, which may either be constant or estimated from $C_f = g/C_z^2$, where C_z is the Chezy factor.

3. MODIFIED SGM FOR A STEP (SGMS)

The authors have proposed a general scheme, the surface gradient method (SGM) [6], for the accurate treatment of source terms such as bed slope in the shallow water equations. In this section, we extend the SGM for flows over a vertical step, which is hereafter referred to SGMS.

3.1. Representation of a vertical step

In order to simulate shallow water flows over a bed topography in which there is discontinuity such as a vertical step, a true representation of the bed should be taken into account in a mathematical model. Without loss of generality, a one-dimensional situation is described here for clarity. Firstly, we define bed topography at cell face points with a linear piecewise profile. Then we use z_b^- and z_b^+ to denote the two values of bed height at the same cell face point, e.g. $z_{bi+1/2}^-$ stands for z_b at left side of the cell face $i + 1/2$ (Point f_-), and $z_{bi+1/2}^+$ stands for z_b at right side of the cell face $i + 1/2$ (Point f_+), as shown in Figure 1. Clearly, with this definition, a bed discontinuity such as a vertical step can be exactly represented with z_b^- and z_b^+. When there is no discontinuity in bed topography, $z_b^- = z_b^+$. Under this definition, the bed height z_b at grid point i is

$$z_{bi} = \frac{(z_{bi+1/2}^- + z_{bi-1/2}^+)}{2} \tag{5}$$

3.2. Data reconstruction at a vertical step interface

Data reconstruction for each conservative variable is necessary in a higher order accurate Godunov-type method. However, there is no existing method which can be used to accurately calculate the left and right data at a cell interface with a vertical step, hence it is unknown how to calculate the corresponding numerical fluxes with a Riemann solver. Below, we described a simple scheme based on the SGM for data reconstruction at a vertical step interface.

In the SGM, the water surface level $\eta(x,t)$ is used as the basis for data reconstruction, i.e.

$$\eta(x,t) = h(x,t) + z_b(x) \quad \text{(see Figure 1)} \tag{6}$$

and a piecewise linear reconstruction is used for η, i.e.

$$\eta = \eta_i + (x - x_i)\delta\eta_i \tag{7}$$

where $\delta\eta_i$ is the gradient of η within cell i (Figure 1), which can be determined by

$$\delta\eta_i = G\left(\frac{\eta_{i+1} - \eta_i}{x_{i+1} - x_i}, \frac{\eta_i - \eta_{i-1}}{x_i - x_{i-1}}\right) \tag{8}$$

in which G is a slope limiter which is used to avoid generating spurious oscillations in the reconstructed data at the cell interface [7]. The slope limiter may take one of the following forms,

(i) Minmod limiter

$$G(a,b) = \max[0, \min(a,b)] \tag{9}$$

(ii) van Leer limiter

$$G(a,b) = \frac{a|b| + |a|b}{|a| + |b|} \tag{10}$$

(iii) Superbee limiter

$$G(a,b) = s\max[0, \min(2|b|, sa), \min(|b|, 2sa)] \tag{11}$$

with $s = sgn(b)$.

The water depth at grid point i is calculated as

$$h_i = \eta_i - z_{bi} \tag{12}$$

and the values of ϕ at the left and right of the cell interface $(i-1/2)$ are accurately calculated as

$$\phi^L_{i-1/2} = g\left(\eta_{i-1} + \frac{1}{2}\Delta x_{i-1}\delta\eta_{i-1} - z_{bi-1/2}\right) \tag{13}$$

and

$$\phi^R_{i-1/2} = g\left(\eta_i - \frac{1}{2}\Delta x_i\delta\eta_i - z_{bi-1/2}\right) \tag{14}$$

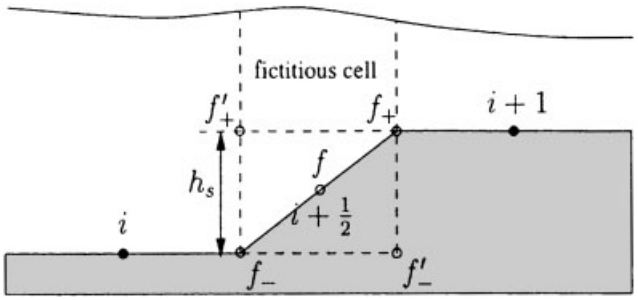

Figure 2. Fictitious cell for vertical step.

As indicated earlier, Equations (13) and (14) can be used to get accurate values of ϕ at cell interfaces for continuous bed topography. To determine the values of ϕ at the vertical step interface, we create a fictitious cell with a slope for the vertical step as shown in Figure 2, i.e. the interface $i+1/2$ is replaced by a fictitious cell f with two cell interface f_- and f_+ (see Figure 2). With the aid of the fictitious cell, using Equations (13) and (14), ϕ^L and ϕ^R for cell i at the interface f_- are

$$\phi^L_{f_-} = g\left(\eta_i + \frac{1}{2}\Delta x_i \delta\eta_i - z_{bf_-}\right) \tag{15}$$

$$\phi^R_{f_-} = g\left(\eta_f - \frac{1}{2}\Delta x_f \delta\eta_f - z_{bf_-}\right) \tag{16}$$

If the fictitious cell is removed, i.e. $\Delta x_f = (x_{f_+} - x_{f_-}) \to 0$ from the right, then $f_+ \to f'_+$, giving

$$\lim_{f_+ \to f'_+}\left(\eta_f - \frac{1}{2}\Delta x_f \delta\eta_f - z_{bf_-}\right) = \eta_{i+1} - \frac{1}{2}\Delta x_{i+1}\delta\eta_{i+1} - z_{bf_-} \tag{17}$$

Substitution of Equation (17) into Equation (16) results in

$$\phi^R_{f_-} = g\left(\eta_{i+1} - \frac{1}{2}\Delta x_{i+1}\delta\eta_{i+1} - z_{bf_-}\right) \tag{18}$$

Notice that $z_{bf_-} = z^-_{bi+1/2}$ when $\Delta x_f = 0$, Equations (15) and (18) are finally written for cell i as

$$\phi^L_{i+1/2} = g\left(\eta_i + \frac{1}{2}\Delta x_i \delta\eta_i - z^-_{bi+1/2}\right) \tag{19}$$

$$\phi^R_{i+1/2} = g\left(\eta_{i+1} - \frac{1}{2}\Delta x_{i+1}\delta\eta_{i+1} - z^-_{bi+1/2}\right) \tag{20}$$

Similarly when cell $i+1$ is considered, the values of ϕ at the left and right of the cell interface $(i+1/2)$ are

$$\phi^L_{i+1/2} = g\left(\eta_i + \frac{1}{2}\Delta x_i \delta\eta_i - z^+_{bi+1/2}\right) \tag{21}$$

$$\phi^R_{i+1/2} = g\left(\eta_{i+1} - \frac{1}{2}\Delta x_{i+1} \delta\eta_{i+1} - z^+_{bi+1/2}\right) \tag{22}$$

3.3. *Effect of a vertical step*

Theoretically, the shallow water equations are not valid for flows over a vertical step due to the assumption of hydrostatic pressure. On the other hand, there is a local head loss where there is sudden change in channel geometry according to theory of open channel hydraulics [8]. If we assume that flows over a vertical step have similar hydraulic characteristics to that through a suddenly contracted channel, the head loss can be calculated by

$$h_\xi = \xi \frac{u^2_{i+1}}{2g} \tag{23}$$

where h_ξ is the local head loss and ξ is an empirical factor for the local head loss.

Since a local head loss is caused by a sudden change in flow geometry, if a vertical step is located at the cell interface $i+1/2$, we may interpret such loss as resistance stress τ_ξ due to the vertical step, i.e.

$$\tau_\xi = \rho g h_\xi = \rho \xi u^2_{i+1} \tag{24}$$

which can be written in the following form for a 2D flow as

$$\tau_{\xi x} = \rho \xi u_{i+1}\sqrt{u^2_{i+1} + v^2_{i+1}}, \qquad \tau_{\xi y} = \rho \xi v_{i+1}\sqrt{u^2_{i+1} + v^2_{i+1}} \tag{25}$$

Therefore, the effect of a vertical step on flows may be taken into account by solving Equation (1) with the modified source terms $\mathbf{S} = \mathbf{S}_b + \mathbf{S}_f + \mathbf{S}_r$ in which $\mathbf{S}_r$ is the resistance stress defined by

$$\mathbf{S}_r = \begin{pmatrix} 0 \\ -\dfrac{g}{\rho}\tau_{\xi x} \\ -\dfrac{g}{\rho}\tau_{\xi y} \end{pmatrix} \tag{26}$$

only for neighbouring cell i or $i+1$ of the vertical step: i.e. when $(z^+_{bi+1/2} - z^-_{bi+1/2}) > 0$, τ_ξ affects only the cell i and the solution with Equation (26) is needed for cell i only; when $(z^+_{bi+1/2} - z^-_{bi+1/2}) < 0$, τ_ξ affects only the cell $i+1$ and the solution with Equation (26) is needed for cell $i+1$ only.

4. MUSCL-HANCOCK METHOD

The SGMS described in Section 3 may be incorporated into any higher order accurate Godunov-type method which requires data reconstruction. Since the MUSCL-Hancock [9] is a second-order accurate, high resolution, upwind scheme of the Godunov-type, it is chosen for the solution of Equation (1). The method consists of a predictor step and a corrector step.

In the predictor step, a non-conservative approach is used to determine the intermediate values over a half time step,

$$(A\mathbf{U})_{ij}^{n+1/2} = (A\mathbf{U})_{ij}^{n} - \frac{\Delta t}{2}\left(\sum_{m=1}^{M} \mathbf{F}(\mathbf{U}_m)^n \cdot \mathbf{L}_m - (A\mathbf{S})_{ij}^{n}\right) \tag{27}$$

where A is the cell area, $\mathbf{L}_m$ is the cell side vector defined as the cell side length multiplied by its outward pointing unit normal vector and $M = 4$ is the number of sides of the cell. The flux vector $\mathbf{F}(\mathbf{U}_m)$ is evaluated at each cell face m following data reconstruction based on neighbouring cell centre data. For the continuity equation, the SGM is used, i.e. the values of ϕ at the cell interfaces $(i - 1/2j)$ and $(i + 1/2j)$ for the cell ij under consideration are expressed using Equations (13) and (14) as

$$\phi_{i-1/2j} = g\left(\eta_{ij} - \frac{1}{2}\Delta x_{ij}\delta\eta_{xij} - z^{+}_{bi-1/2j}\right) \tag{28}$$

and

$$\phi_{i+1/2j} = g\left(\eta_{ij} + \frac{1}{2}\Delta x_{ij}\delta\eta_{xij} - z^{-}_{bi+1/2j}\right) \tag{29}$$

For the momentum equations, a piecewise linear reconstruction is used to calculate the values of ϕu and ϕv at cell interfaces. For example, ϕu and ϕv at the cell interfaces $(i - 1/2j)$ and $(i + 1/2j)$ can be calculated as

$$(\phi u)_{i-1/2j} = (\phi u)_{ij} - \frac{1}{2}\Delta x_{ij}\delta(\phi u)_{xij} \tag{30}$$

$$(\phi u)_{i+1/2j} = (\phi u)_{ij} + \frac{1}{2}\Delta x_{ij}\delta(\phi u)_{xij} \tag{31}$$

and

$$(\phi v)_{i-1/2j} = (\phi v)_{ij} - \frac{1}{2}\Delta x_{ij}\delta(\phi v)_{xij} \tag{32}$$

$$(\phi v)_{i+1/2j} = (\phi v)_{ij} + \frac{1}{2}\Delta x_{ij}\delta(\phi v)_{xij} \tag{33}$$

where $\delta(\phi u)_{xij}$ and $\delta(\phi v)_{xij}$ are the gradients of ϕu and ϕv in the x direction within the cell ij, respectively. They are calculated in the same way as $\delta\eta_i$.

In the corrector step, a fully conservative solution over a full time step is achieved by solving a series of local Riemann problems based on data from the predictor step,

$$(A\mathbf{U})_{ij}^{n+1} = (A\mathbf{U})_{ij}^{n} - \Delta t \left(\sum_{m=1}^{M} \mathbf{F}(\mathbf{U}_m^L, \mathbf{U}_m^R)^{n+1/2} \cdot \mathbf{L}_m - (A\mathbf{S})_{ij}^{n+1/2} \right) \tag{34}$$

where the flux vector $\mathbf{F}(\mathbf{U}_m^L, \mathbf{U}_m^R)$ is calculated by solving a local Riemann problem at each cell interface. $\mathbf{U}_m^L$ and $\mathbf{U}_m^R$ are vectors of the conservative variables at the left and right sides of cell interface m, defined by expressions such as Equation (13) for ϕ and expressions similar to Equations (30), (31), (32) and (33) for ϕu and ϕv, respectively. It must be noted that at neighbouring cells of the vertical step the left and right values of ϕ should be calculated with expressions such as Equations (19) and (20) for the cell ij if the vertical step is located at $i + 1/2j$.

In the present study, the HLL approximate Riemann solver [10] (see Figure 3) is used to calculate the fluxes $\mathbf{F}(\mathbf{U}_m^L, \mathbf{U}_m^R)$, i.e. the flux at the cell interface $i + 1/2$ is determined by

$$\mathbf{F}(\mathbf{U}_m^L, \mathbf{U}_m^R) = \begin{cases} \mathbf{F}(\mathbf{U}_m^L) & \text{if } s_L \geqslant 0 \\ \mathbf{F}^*(\mathbf{U}_m^L, \mathbf{U}_m^R) & \text{if } s_L < 0 < s_R \\ \mathbf{F}(\mathbf{U}_m^R) & \text{if } s_R \leqslant 0 \end{cases} \tag{35}$$

where

$$\mathbf{F}^*(\mathbf{U}_m^L, \mathbf{U}_m^R) = \frac{s_R \mathbf{F}(\mathbf{U}_m^L) - s_L \mathbf{F}(\mathbf{U}_m^R) + s_L s_R (\mathbf{U}_m^R - \mathbf{U}_m^L)}{s_R - s_L} \tag{36}$$

with wave speeds s_L and s_R defined by

$$s_L = \min(\mathbf{V}^L \cdot \vec{n}_m - \sqrt{\phi^L}, u_s - \sqrt{\phi_s}) \tag{37}$$

$$s_R = \max(\mathbf{V}^R \cdot \vec{n}_m + \sqrt{\phi^R}, u_s + \sqrt{\phi_s}) \tag{38}$$

in which u_s and ϕ_s are estimated as [11]

$$u_s = \frac{1}{2}(\mathbf{V}^L + \mathbf{V}^R) \cdot \vec{n}_m + \sqrt{\phi^L} - \sqrt{\phi^R} \tag{39}$$

$$\sqrt{\phi_s} = \frac{\sqrt{\phi^L} + \sqrt{\phi^R}}{2} + \frac{(\mathbf{V}^L - \mathbf{V}^R) \cdot \vec{n}_m}{4} \tag{40}$$

and $\vec{n}_m$ is the normalized side vector for cell face m.

It may be noted that the expressions (37) and (38) for a dry bed problem are modified as [12]

$$s_L = \mathbf{V}^L \cdot \vec{n}_m - \sqrt{\phi^L}, \quad s_R = \mathbf{V}^L \cdot \vec{n}_m + 2\sqrt{\phi^L} \quad \text{(Right dry bed)} \tag{41}$$

and

$$s_L = \mathbf{V}^R \cdot \vec{n}_m - 2\sqrt{\phi^R}, \quad s_R = \mathbf{V}^R \cdot \vec{n}_m + \sqrt{\phi^R} \quad \text{(Left dry bed)} \tag{42}$$

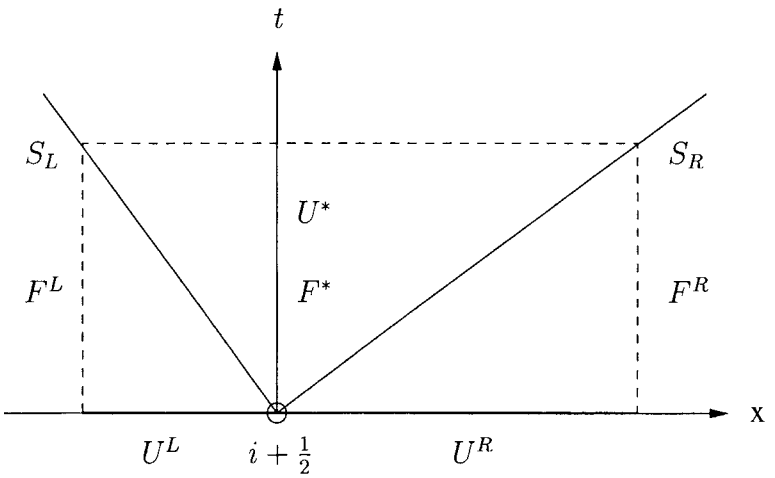

Figure 3. HLL approximate Riemann solver.

Although the SGMS described in Section 3 is generally suitable for both uniform and non-uniform meshes, a uniform Cartesian mesh is used here to maintain the same computational conditions as that reported in the literature. The time step Δt is calculated at the start of each time step by

$$\Delta t = C_t \min(\Delta t_x, \Delta t_y) \tag{43}$$

where

$$\Delta t_x = \min_i \frac{\Delta x}{|u_{ij}| + \sqrt{\phi_{ij}}}, \qquad \Delta t_y = \min_j \frac{\Delta y}{|v_{ij}| + \sqrt{\phi_{ij}}} \tag{44}$$

in which C_t is the Courant number ($0 < C_t \leqslant 1$). To test the robustness of the scheme, three values, 0.3, 0.65 and 1, were used for C_t in all the numerical computations presented here, and no stability problems were encountered. However, a value of $C_t \leqslant 0.95$ gives accurate results in all the present computations.

5. FEATURES OF THE PROPOSED SCHEME

5.1. Conservative property

The numerical scheme proposed in Section 3 satisfies the $\mathscr{Z}$-property [6], i.e. it provides the exact values of variables in the flow domain for the stationary case $h \equiv H$, $\mathbf{V} \equiv 0$; and replicates the exact solution to the stationary flow problem defined by

$$h \equiv H, \qquad \mathbf{V} \equiv 0 \tag{45}$$

for which there are non-vanishing terms in the momentum equations due to bed topography,

$$\frac{\partial}{\partial x}\left(\frac{1}{2}\phi^2\right) = g\phi\frac{\partial H}{\partial x}, \qquad \frac{\partial}{\partial y}\left(\frac{1}{2}\phi^2\right) = g\phi\frac{\partial H}{\partial y} \tag{46}$$

This is a very desirable feature for a numerical method and the latter is referred as the $\mathscr{C}$-property in literature [1].

The proof for the case of continuous bed topography is given by Zhou *et al.* [6]. Here we give the proof for a cell with a vertical step for the one-dimensional case. This may be applied to two-dimensional cases in an analogous manner.

Assuming a vertical step is located at cell face $i+1/2$, i.e.

$$z^+_{bi+1/2} = z^-_{bi+1/2} + h_s \quad \text{(see Figure 1)} \tag{47}$$

For cell i, only the interface $i+1/2$ needs special treatment and Equations (19) and (20) are used to decide $\phi^L_{i+1/2}$ and $\phi^R_{i+1/2}$ as

$$\phi^L_{i+1/2} = g\left(\eta_i + \frac{1}{2}\Delta x_i \delta\eta_i - z^-_{bi+1/2}\right) = g(\eta_i - z^-_{bi+1/2}) = gh^-_{i+1/2} \tag{48}$$

$$\phi^R_{i+1/2} = g\left(\eta_{i+1} - \frac{1}{2}\Delta x_{i+1} \delta\eta_{i+1} - z^-_{bi+1/2}\right) = g(\eta_{i+1} - z^-_{bi+1/2}) = gh^-_{i+1/2} \tag{49}$$

because $\delta\eta = 0$ and $\eta_i = \eta_{i+1}$ with the initial stationary condition (45). This gives the wave speeds from Equations (37) and (38) as

$$s_L = -\sqrt{gh^-_{i+1/2}}, \qquad s_R = \sqrt{gh^-_{i+1/2}} \tag{50}$$

where the superscript '$-$' indicates the left value of a variable at the vertical cell interface and superscript '$+$' the right value at the same interface. This notation is subsequently used throughout this paper.

In the predictor step, the x component of numerical flux, F_x, is

$$F_x = \frac{[\phi(u^2 + \frac{1}{2}\phi)]^-_{i+1/2} - [\phi(u^2 + \frac{1}{2}\phi)]^+_{i-1/2}}{\Delta x} = \frac{1}{2} g^2 \frac{(h^-_{i+1/2} + h^+_{i-1/2})(h^-_{i+1/2} - h^+_{i-1/2})}{\Delta x} \tag{51}$$

because $u \equiv 0$ and $\phi = gh$.

It should be noted that the water level is constant under the initial condition $h \equiv H$ and $u \equiv 0$, in which there is no local head loss, i.e. $\tau_\xi = 0$. Data reconstruction with the SGM/SGMS provides zero gradient ($\delta\eta = 0$) for the water level in the whole domain; hence the method gives the exact values of depth h or ϕ in the whole domain.

Since

$$h^+_{i-1/2} = \eta_{i-1/2} - z^+_{bi-1/2} = \eta_i - \frac{1}{2}\Delta x \delta\eta_i - z^+_{bi-1/2} \tag{52}$$

and

$$h^-_{i+1/2} = \eta_{i+1/2} - z^-_{bi+1/2} = \eta_i + \frac{1}{2}\Delta x \delta\eta_i - z^-_{bi+1/2} \tag{53}$$

we have

$$\frac{(h^-_{i+1/2} + h^+_{i-1/2})}{2} = \eta_i - \frac{(z^-_{bi+1/2} + z^+_{bi-1/2})}{2} = (\eta_i - z_{bi}) + z_{bi} - \frac{(z^-_{bi+1/2} + z^+_{bi-1/2})}{2} \tag{54}$$

Noting that $(\eta_i - z_{bi}) = h_i$ and Equation (5), Equation (54) becomes

$$\frac{(h^-_{i+1/2} + h^+_{i-1/2})}{2} = h_i \tag{55}$$

Substitution of Equation (55) into Equation (51) results in

$$F_x = g^2 h_i \frac{(h^-_{i+1/2} - h^+_{i-1/2})}{\Delta x} \tag{56}$$

On the other hand, the x component of the bed slope source term may be discretized with a centred scheme as

$$S_x = g\phi_i \frac{H^-_{i+1/2} - H^+_{i-1/2}}{\Delta x} = g^2 h_i \frac{h^-_{i+1/2} - h^+_{i-1/2}}{\Delta x} = F_x \tag{57}$$

because $h \equiv H$. This proves that the numerical scheme in the predictor step satisfies the exact $\mathscr{C}$-property, hence $h \equiv H$ and $u \equiv 0$ are preserved after the predictor step.

In the corrector step, the numerical flux at the right-hand interface, $F_{i+1/2}$, is defined by Equation (35),

$$F_{i+1/2} = \frac{s_R[\phi(u^2 + \frac{1}{2}\phi)]^L_{i+1/2} - s_L[\phi(u^2 + \frac{1}{2}\phi)]^R_{i+1/2} + s_L s_R[(\phi u)^R_{i+1/2} - (\phi u)^L_{i+1/2}]}{s_R - s_L} \tag{58}$$

because $s_L < 0 < s_R$.

Since up to this point $h \equiv H$ and $u \equiv 0$, which leads to $\tau_\xi = 0$, have been maintained over the whole domain, ϕ can also be obtained exactly with the SGM/SGMS and no discontinuity in water surface will appear anywhere in the domain, i.e. $\eta^L \equiv \eta^R$ at all the cell interfaces. Substitution of Equations (48)–(50) and $u \equiv 0$ into the above equation gives

$$F_{i+1/2} = \frac{\frac{1}{2}\sqrt{gh^-_{i+1/2}}(\phi^-_{i+1/2})^2 + \frac{1}{2}\sqrt{gh^-_{i+1/2}}(\phi^-_{i+1/2})^2}{2\sqrt{gh^-_{i+1/2}}} = \frac{1}{2}(\phi^-_{i+1/2})^2 \tag{59}$$

Similarly, we have

$$F_{i-1/2} = \frac{1}{2}(\phi^+_{i-1/2})^2 \tag{60}$$

The numerical flux is

$$F_x = \frac{F_{i+1/2} - F_{i-1/2}}{\Delta x} = \frac{\frac{1}{2}(\phi^-_{i+1/2})^2 - \frac{1}{2}(\phi^+_{i-1/2})^2}{\Delta x} = \frac{1}{2} g^2 \frac{(h^-_{i+1/2} + h^+_{i-1/2})(h^-_{i+1/2} - h^+_{i-1/2})}{\Delta x} \tag{61}$$

which has exactly the same form as Equation (51) in the predictor step with the same initial conditions (45). It then follows that the corrector step also satisfies the exact $\mathscr{C}$-property. Again, $h \equiv H$ and $u \equiv 0$ are preserved after the corrector step.

The proof for cell $i+1$ can be similarly formulated. Therefore, the proposed scheme satisfies the $\mathscr{Z}$-property for bed topography with a discontinuity.

5.2. Discretization of source term

The centred discretization is applied for all the source terms. Since a vertical step is taken into account, the bed slope term for cell ij is discretized in the following general form,

$$\int\int_{\Delta x\Delta y} g\phi \frac{\partial H}{\partial x}\,\mathrm{d}x\,\mathrm{d}y = \int\int_{\Delta x\Delta y} -g\phi \frac{\partial z_b}{\partial x}\,\mathrm{d}x\,\mathrm{d}y = -g\Delta y\phi_{ij}(z^{-}_{bi+1/2j} - z^{+}_{bi-1/2j}) \tag{62}$$

which is suitable for bed topography with or without a discontinuity such as a vertical step, preserving the second-order accuracy.

6. VALIDATION OF THE SCHEME

To verify the proposed scheme, we solve some benchmark problems. The numerical results are compared with either analytical solutions or available experimental data, demonstrating the capability and accuracy of the method.

6.1. A surge crossing a step

A surge crossing a step is simulated here. The channel is 1000 m long with a step of height $h_s = 2$ m located in the middle of the channel as shown in Figure 4. This is the same as that used by Hu *et al.* [5] who replaced the step with a steep bed slope. In the numerical computation 400 uniform cells with $\Delta x = 25$ m were used. Assuming the step is located at cell interface $i + 1/2$, i.e. $(z^{+}_{bi+1/2} - z^{-}_{bi+1/2}) = h_s$, the factor ξ for the solution of cell i is estimated from

$$\xi = 0.5\left(\frac{\phi_i - \phi_{i+1}}{\phi_i}\right) \tag{63}$$

The initial conditions are: (i) the water depth at upstream end is 10 m, (ii) the water surface is $\eta = 5$ m in the channel, and (iii) the velocity of the surge at the entrance is defined using the theory of open channel hydraulics [8] as

$$u(0,t) = (\eta_u - \eta_d)\sqrt{\frac{g(\eta_u + \eta_d)}{2\eta_u\eta_d}} \tag{64}$$

where $\eta_u = 10$ m and $\eta_d = 5$ m.

Figures 4 and 5 depict comparisons between the numerical results and analytical solutions given by Chow [8], which show very good agreement. This suggests that the proposed scheme is able to simulate a surge crossing a step.

6.2. A tidal wave flow over steps

A tidal wave flow over a bed with two steps as shown in Figure 6 is next considered. The bed profile was proposed at a workshop on dam-break wave simulations [13] and defined

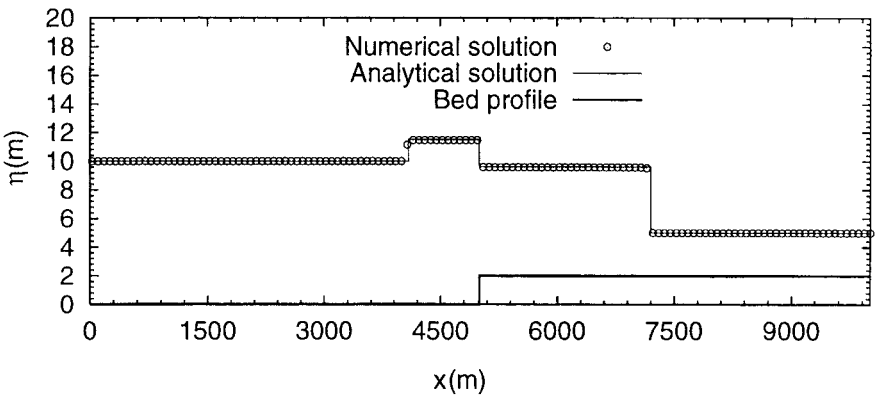

Figure 4. Surge crossing a step: comparison of water surface at $t = 600.5$ s.

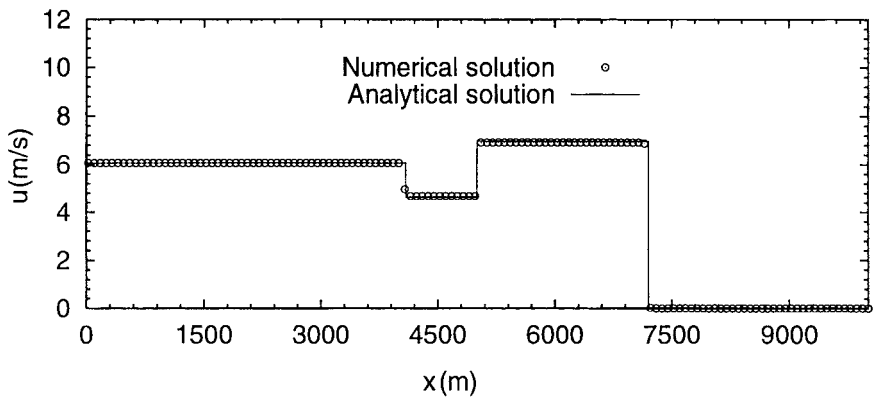

Figure 5. Surge crossing a step: comparison of velocity at $t = 600.5$ s.

by

$$z_b(x) = \begin{cases} 8 & \text{if } |x - \dfrac{1500}{2}| \leqslant \dfrac{1500}{8} \\ 0 & \text{otherwise} \end{cases} \tag{65}$$

and the channel is 1500 m long.

The initial and boundary conditions are

$$h(x, 0) = H(x) \tag{66}$$

$$u(x, 0) = 0 \tag{67}$$

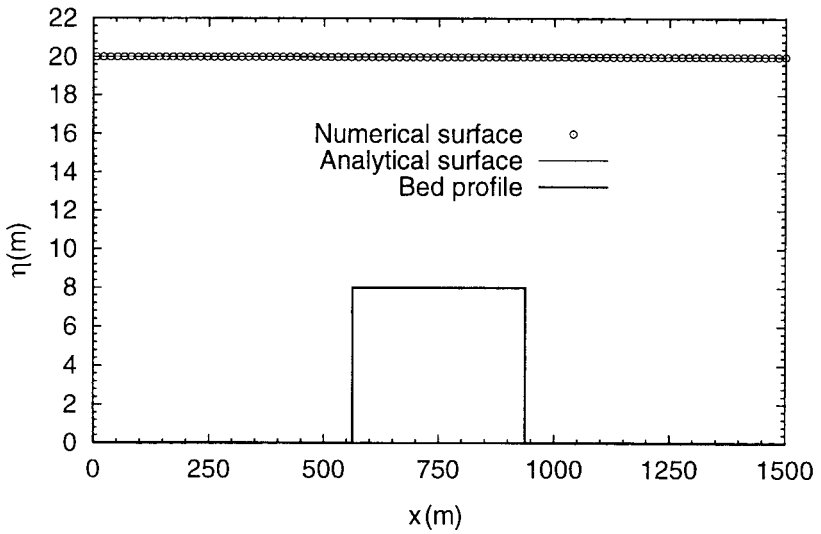

Figure 6. A tidal wave: comparison of water surface η at $t = 10\,800$ s.

and

$$h(0,t) = H(0) + 4 - 4\sin\left[\pi\left(\frac{4t}{86\,400} + \frac{1}{2}\right)\right] \tag{68}$$

$$u(L,t) = 0 \tag{69}$$

where $H(x) = H(0) - z_b(x)$ with $H(0) = 16$ m and $L = 1500$ m is the channel length.

Under these conditions, the tidal wave is a relatively short and an asymptotic analytical solution is derived by Bermudez and Vázquez [1] as

$$h(x,t) = H(x) + 4 - 4\sin\left[\pi\left(\frac{4t}{86\,400} + \frac{1}{2}\right)\right] \tag{70}$$

$$u(x,t) = \frac{(x-L)\pi}{5400h(x,t)}\cos\left[\pi\left(\frac{4t}{86\,400} + \frac{1}{2}\right)\right] \tag{71}$$

In the computations, a total of 200 grid points were used with $\Delta x = 7.5$ m, in which the two steps are located at $x_1 = (76 + 1/2)\Delta x$ and $x_2 = (126 + 1/2)\Delta x$, respectively. When solution is taken for cell $i = 76$, the factor ξ is

$$\xi_1 = 0.5\left(\frac{\phi_i - \phi_{i+1}}{\phi_i}\right) \tag{72}$$

and for cell $i = 127$ the factor ξ is

$$\xi_2 = 0.5\left(\frac{\phi_{i-1} - \phi_i}{\phi_{i-1}}\right) \tag{73}$$

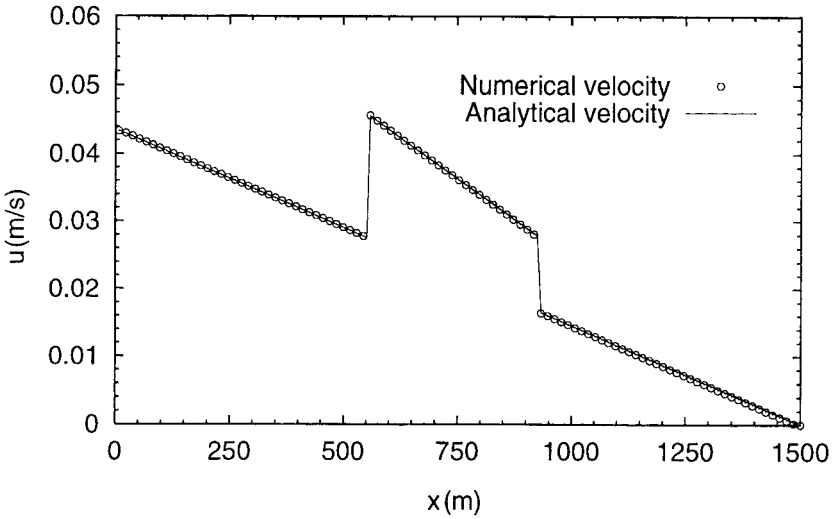

Figure 7. A tidal wave: comparison of velocity u at $t = 10\,800$ s.

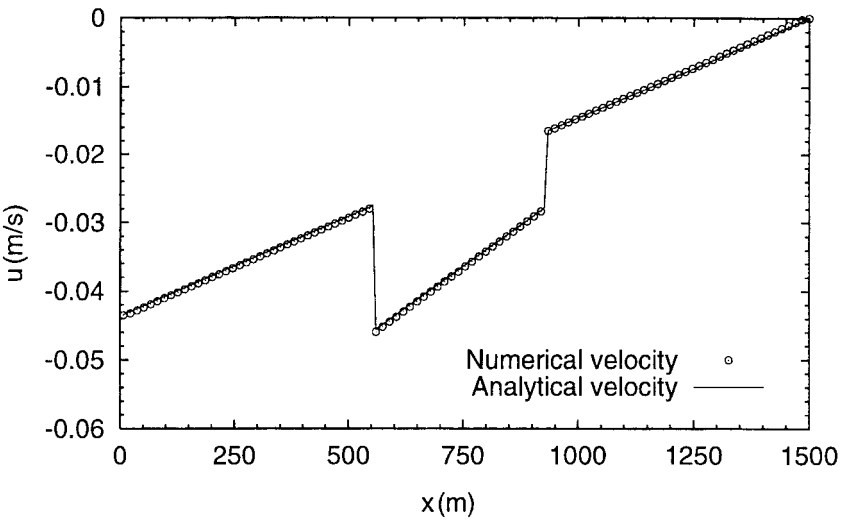

Figure 8. A tidal wave: comparison of velocity u at $t = 32\,400$ s.

Equations (66)–(69) were used as the initial and boundary conditions. Results at $t = 10\,800$ s and $t = 32\,400$ s, corresponding to the half-risen tidal flow with maximum positive velocities and to the half-ebb tidal flow with maximum negative velocities, are compared with the asymptotic analytical solutions in Figures 6–8, showing an excellent agreement. This indicates that the proposed scheme is accurate for tidal flow over a bed with steps.

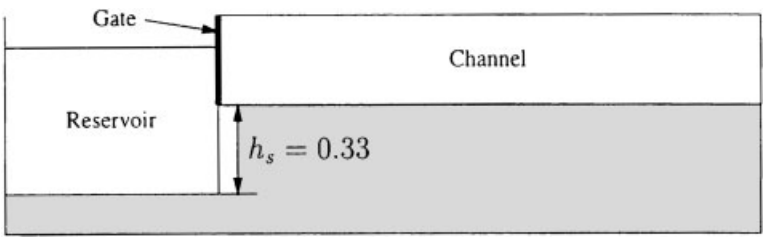

Figure 9. Geometry of the reservoir and L-shaped channel: side view.

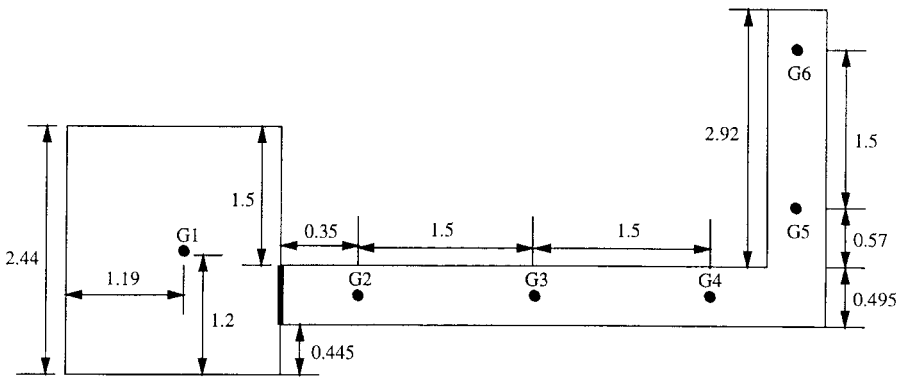

Figure 10. Geometry of the reservoir and L-shaped channel: plan view.

6.3. *Dam-break flows*

This test problem is the experimental case designed by the CADAM team [14] for verifying the capability of numerical methods to simulate dam-break flows. The flow domain consists of a square reservoir and L-shaped channel as shown in Figures 9 and 10. The bed of the reservoir is 0.33 m below that of the channel which forms a vertical step at the entrance to the channel. Initially, the water depth was 0.53 m high in the reservoir which is separated by a gate from the channel and then the gate is suddenly opened to produce a dam-break situation. The Manning's friction coefficient for the bed is $0.0095\ \mathrm{s\,m^{-1/3}}$. Two cases, i.e. a wet-bed and a dry-bed case, were studied here. For a wet-bed in the channel, the depth was set to 0.01 m and for a dry-bed, the depth in the channel was set to zero.

In the numerical computations, a mesh with $\Delta x = 0.05017\,\mathrm{m}$ and $\Delta y = 0.0495\,\mathrm{m}$ was used, which corresponds to a total of 138×79 cells. The factor ξ for the local head loss caused by the vertical step is estimated from

$$\xi = 0.5\left(\frac{\phi_i - \phi_{i+1}}{\phi_i}\right) \tag{74}$$

which is used for the solution of the cell i on the condition that $(z^{+}_{bi+1/2} - z^{-}_{bi+1/2}) = h_s$.

According to hydraulics, where there is sudden change in flow geometry, there is local head loss. Since a dam-break flow occurs at the entrance to the channel from the reservoir,

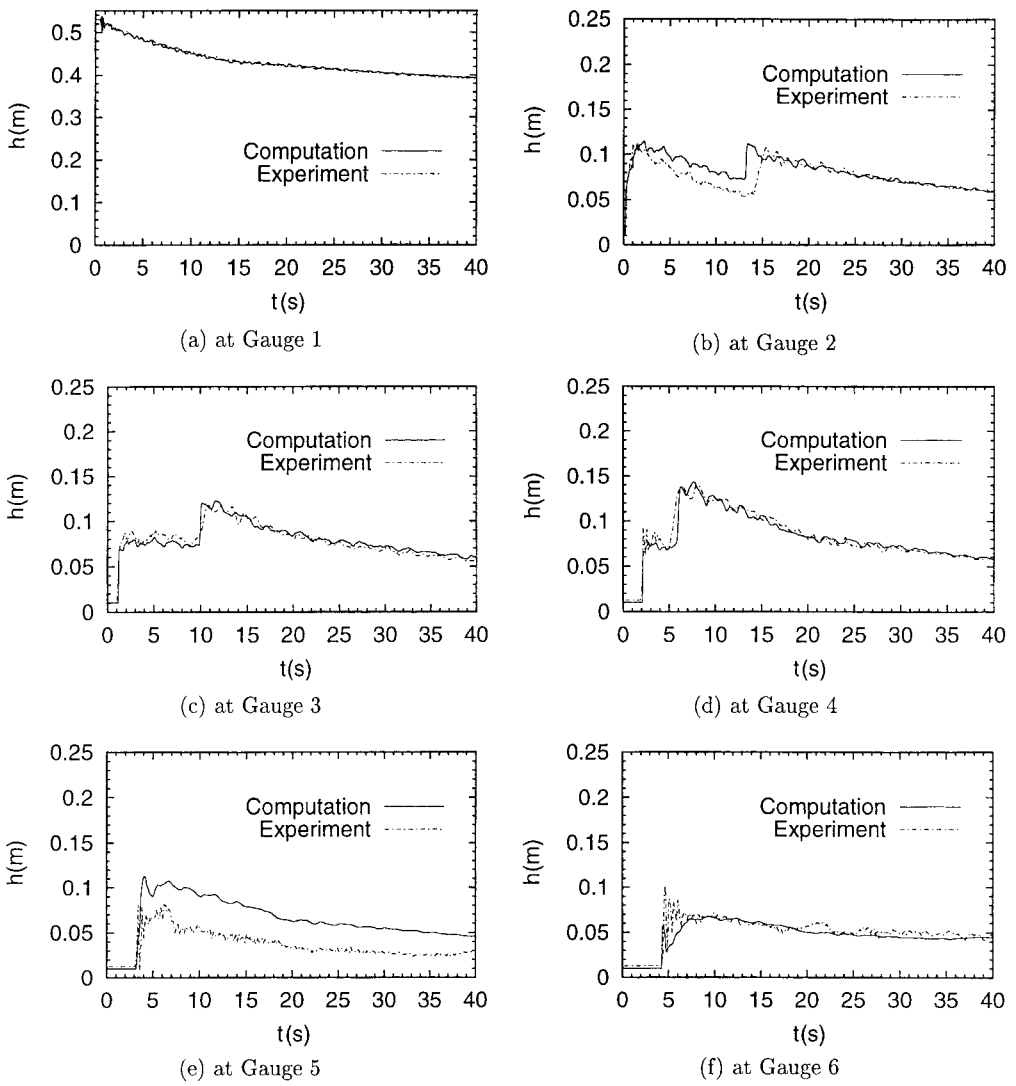

Figure 11. Dam-break flows on wet-bed: comparisons of water depth.

there is sudden contraction in the horizontal flow domain (see the plan view of the domain in Figure 10). This will cause an additional local head loss to that caused by the vertical step. In a similar way to that for the local head loss at a sudden contraction, the head loss can be estimated in an analogous way to Equation (25) derived in Section 3.3 using another loss factor ξ_c given by

$$\xi_c = 0.5\left(\frac{W_r - W_c}{W_c}\right) \tag{75}$$

where $W_r = 2.44$ m is the width of the reservoir and $W_c = 0.495$ m is the channel width.

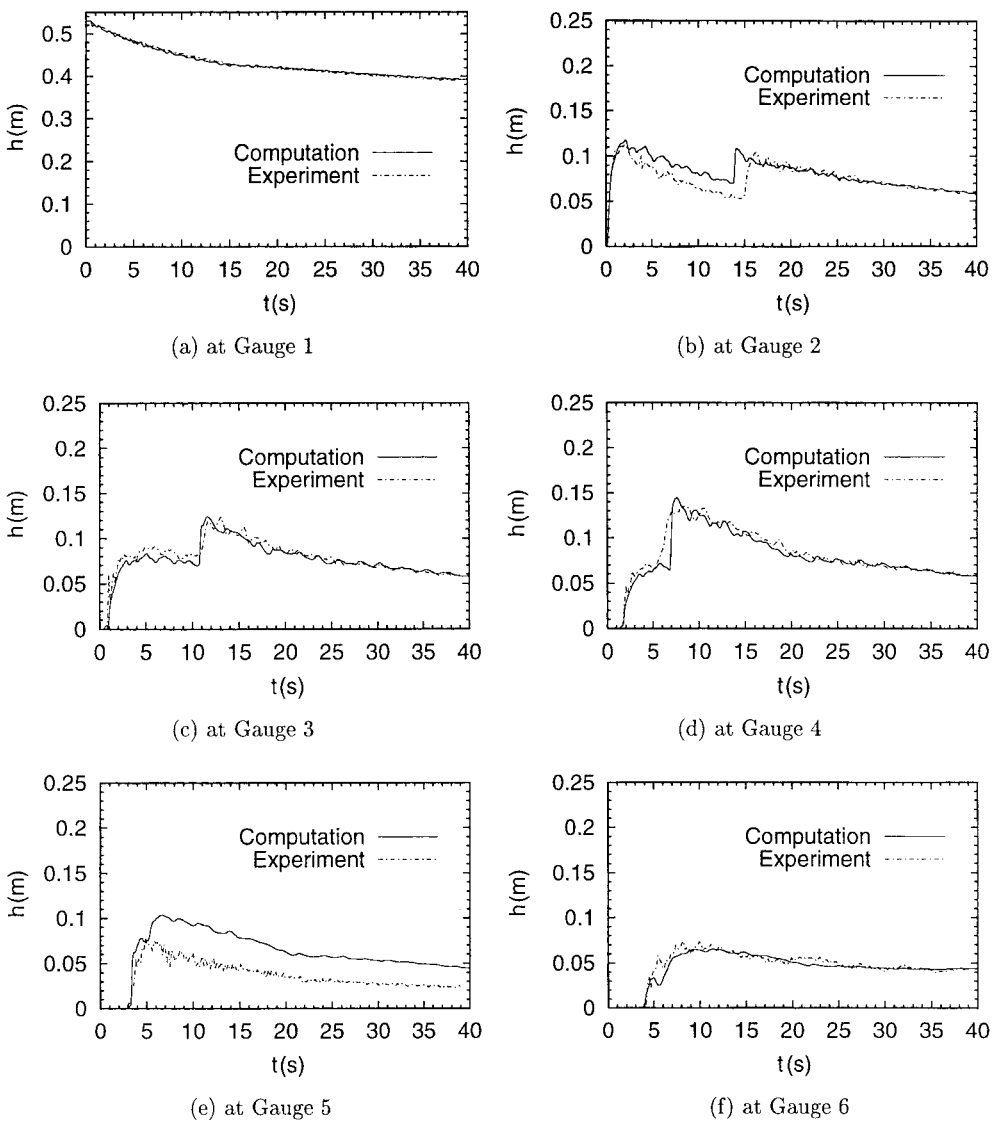

Figure 12. Dam-break flows on dry-bed: comparisons of water depth.

This head loss is also taken into account when the solution is obtained at cell i, supposing $(z^{+}_{bi+1/2} - z^{-}_{bi+1/2}) = h_s$. The variation of water depth with time is compared with the experimental data at the different gauge positions as shown in Figures 11 and 12 for the wet-bed and dry-bed cases, respectively. At most gauge positions, there is good agreement with the experimental data.

However, there are differences at Gauge 2 and Gauge 5. The overall disagreement at Gauge 5 may be due to the further local head loss caused by the 90° bend which is not taken into

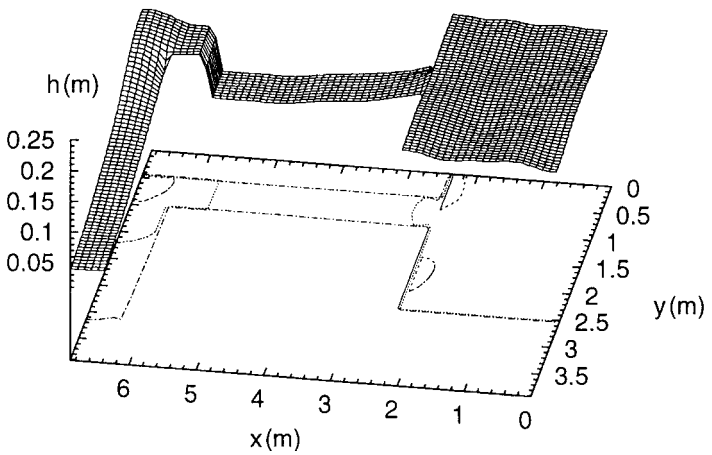

Figure 13. Dam-break flows on wet-bed: 3D plot of the water surface at $t = 6.25$ s.

account in the numerical computations. A 3D plot of the water surface with respect to the channel bed is depicted in Figure 13, showing the complicated flow phenomena.

7. CONCLUSIONS

The authors' SGM is extended to treat a vertical step for shallow water flows. The method retains the conservative property and provides accurate values of conservative variables at cell interface at a vertical step; hence the fluxes at the cell interface can accurately be calculated with a Riemann solver. This can be used in any high resolution Godunov-type method which requires data reconstruction. The scheme has been verified by simulating several shallow water flows involving a vertical step. The results have shown that the treatment can provide accurate solutions which show excellent agreement with the corresponding analytical solutions. The method is simple, efficient and robust.

ACKNOWLEDGEMENTS

Funding from the Manchester Metropolitan University, U.K. is gratefully acknowledged.

REFERENCES

1. Bermudez A, Vázquez ME. Upwind methods for hyperbolic conservation laws with source terms. *Computers and Fluids* 1994; **23**:1049–1071.
2. Vázquez-Cendón ME. Improved treatment of source terms in upwind schemes for shallow water equations in channels with irregular geometry. *Journal of Computational Physics* 1999; **148**:497–526.
3. LeVeque RJ. Balancing source terms and flux gradients in high-resolution Godunov methods: the quasi-steady wave-propagation algorithm. *Journal of Computational Physics* 1998; **146**:346–365.
4. Hubbard ME, Garcia-Navarro P. Flux difference splitting and the balancing of source terms and flux gradients. *Journal of Computational Physics* 2001; **165**:89–125.
5. Hu K, Mingham CG, Causon DM. Numerical simulation of wave overtopping of coastal structures using the non-linear shallow water equations. *Coastal Engineering* 2000; **41**:433–465.

6. Zhou JG, Causon DM, Mingham CG, Ingram DM. The surface gradient method for the treatment of source terms in the shallow water equations. *Journal of Computational Physics* 2001; **168**:1–25.
7. Toro EF. *Riemann Solvers and Numerical Methods for Fluid Dynamics.* Springer-Verlag: Berlin, Heidelberg, 1997.
8. Chow VT. *Open-channel Hydraulics.* McGraw-Hill Book Company: New York, 1959.
9. van Leer B. On the relation between the upwind-differencing schemes of Godunov, Enguist-Osher and Roe. *SIAM Journal of Science and Statistical Computations* 1985; **5**(1):1–20.
10. Harten A, Lax PD, van Leer B. On upstream differencing and Godunov-type schemes for hyperbolic conservation laws. *SIAM Review* 1983; **25**(1):35–61.
11. Toro EF. Riemann problems and the WAF method for solving two-dimensional shallow water equations. *Philosophical Transactions of the Royal Society of London*, *A* 1992; **338**:43–68.
12. Fraccarollo L, Toro EF. Experimental and numerical assessment of the shallow water model for two-dimensional dam-break type problems. *Journal of Hydraulic Research* 1995; **33**:843–864.
13. Goutal N, Maurel F (eds). *Proceedings of the 2nd Workshop on Dam-break Wave Simulation*. HE-43/97/016/B. Département Laboratoire National d'Hydraulique, Groupe Hydraulique Fluviale, Electricité de France, France, 1997.
14. *Proceedings of the CADAM meeting*. HR Wallingford, U.K., 2–3 March, 1998.

